Chemical Engineering Journal 431 (2022) 133449

Contents lists available at ScienceDirect

Chemical Engineering Journal

journal homepage: www.elsevier.com/locate/cej

Highly sensitive AIE-based mechanoresponsive luminescent polymer coatings for surface pressure imaging

Di Yang [a,c,1], Yingying Ren [a,1], Jiwei Li [a,b], Qiu Wang [b,*], Xuebing Li [c,*], Xiaozhong Qu [a,*]

[a] Center of Materials Science and Optoelectronics Engineering, College of Materials Science and Opto-Electronic Technology, University of Chinese Academy of Sciences, Beijing 100049, China
[b] State Key Laboratory of High Temperature Gas Dynamics, Institute of Mechanics, Chinese Academy of Sciences, Beijing 100190, China
[c] Key Laboratory of Biofuels, Qingdao Institute of Bioenergy and Bioprocess Technology, Chinese Academy of Science, Qingdao 266101, China

ARTICLE INFO

Keywords:
Pressure sensitive coating
2D optical sensor
Mechanoluminescent
Aggregation induced emission
Hydrostatic and hydrodynamic measurements

ABSTRACT

Herein, we report on a facile methodology for the development of aggregation induced emission (AIE)-based mechanoresponsive luminescent (MRL) polymer coatings with the characteristics of high sensitivity and high reversibility in 2D surface pressure imaging. Amorphous nitro-functionalized tetraphenyethylene was embedded into an elastomer substrate to prevent the crystallization of the dye and meanwhile to allow the conformational variation in response to the gradual deformation and relaxation of the polymer network. The strategy endows strain-mediated fluorescence enhancement and fast recovery of the material in compressive force loading–unloading cycles. The relationship between pressure and fluorescence intensity of the AIE-based MRL coatings was calibrated which showed adjustable sensitivity within kilopascal (kPa) to megapascal (MPa) range, according to the mechanical property of the polymer matrix. The coatings were capable for the detection of surface pressure distribution through non-contact optical observation technique in both static and dynamic processes. The high sensitivity realized the utility of AIE-based materials in the field of hydrodynamics and probably for other applications in industry.

1. Introduction

Non-contact optical sensing of surface pressure distribution has earn continuous attentions in various fields like aircraft design, medical diagnosis, environmental monitoring and mechanical manufacturing [1–7], because of its noninvasive characteristic [8], high resolution and fast responsiveness in two dimensions (2D) [9]. For example, pressure sensitive coatings, generated from pressure sensitive paints (PSP), have been extremely studied for the applications in aerodynamics [10], however, are limited for utilizing in anaerobic environments such as underwater condition because the technique is based on the oxygen quenching of luminescence [11]. Instead, mechanochromic (MC) and mechanoluminescent (ML) materials become attractive candidates in the development of pressure sensors in response to the mechanical properties of local environment [12–15]. So far mechanoresponsive luminogens involve chemical compounds or chemical moieties that enable to alternate their structure or solid-state morphology upon the external energy input, such as shearing, grinding and rubbing etc [14,15]. Among those materials, aggregation induced emission (AIE) luminogens (AIEgens) are receiving increasing interests due to their strong fluorescence in solid state [16]. Besides, the mechanism for fluorescence enhancement of AIEgens is normally attributed to the restriction of intramolecular motions (RIM) which endows them to be ideal optical indicators for visualizing the microenvironmental stimuli that are affecting the structures and properties of the materials [8]. However, a key problem with the AIE-based mechanoresponsive luminescent (MRL) materials for industrial pressure sensing is the lack of reversibility [12]. It is known that most of the MRL materials require external stimuli like thermal annealing, solvent fuming or the alternation of solvents to recover the original fluorescence after exposure to mechanical stimulus [12,15,17–22]. Comparably, the number of examples with self-recovery ability, especially those with rapid dynamics, is much less [23–33].

Among the AIEgens, tetraphenyethylene (TPE) has a propeller-like conformation, which endows favorable RIM effect to grant the AIE activity [34]. Recently, Zhao et. al. reported a derivative of TPE with nitro

* Corresponding authors.
E-mail addresses: wangqiu@imech.ac.cn (Q. Wang), lixb@qibebt.ac.cn (X. Li), quxz@ucas.ac.cn (X. Qu).
[1] D. Yang and Y. Ren contributed equally to this work.

https://doi.org/10.1016/j.cej.2021.133449
Received 8 September 2021; Received in revised form 16 October 2021; Accepted 1 November 2021
Available online 9 November 2021

substituents, emitting AIE fluoresces in amorphous solid state, but not from their crystals due to the trigger of non-irradiative intersystem crossing (ISC) by the packing of nitrophenyl groups [12]. This characteristic brought intrinsic advantages to gain mechano-responsiveness, contributing to an on–off switching of mechanoluminescence, because the crystal of the dye has a loosely packed structure which can be easily broken by mechanical force and then transfer back to amorphous state [15,35]. However, such MRL performance is thermodynamically driven, achieved via phase transition [36]. Except the irreversibility, the phase transition process may also interrupt the continuity of the fluorescence response and therefore affects the quantitative measurement of stress. In addition, the crystalline-to-amorphous switching in the solid phase commonly requires strong force up to gigapascals (GPa) [15,23,37,38]. To extend the application of AIEgens in pressure sensing, new strategies for managing the photophysical process of the luminogens are necessary.

Embedding AIEgens in a polymer matrix is an intelligent choice to design MRL materials [8,14,39]. With a polymer matrix, AIE-active probes can be facilely engineered into films and coatings. In this case, the polymer chains enable to fill the gap or occupy the free volume around the dye molecules to prevent the non-radiative decay [40]. And the crystallization of the organic compounds can be confined by the surrounding polymer chains [41–43]. Thus, we presumed in an elastic network, when phase transition is prohibited whereas the variation of intermolecular distance of AIEgens can be induced by the deformation of the polymer meshes, the molecular motion and hence the photoluminescence property of the AIEgens would correlate to the strain of the polymer matrix. And this would allow the imaging of the surface pressure distribution through the change of local morphology of the polymer. As a proof-of-concept work, we used tetra(4-nitrophenyl) ethylene (TPE-4N, Fig. 1**a**), an AIEgen that is highly emissive in its amorphous aggregate form, to incorporate a poly(dimethylmethylvinylsiloxane) (PDMS) elastomer to construct pressure sensitive coatings. We will demonstrate that the coatings have a desirable characteristic of pressure-induced fluorescence enhancement, besides the mechanoluminescence performance is highly reversible and highly sensitive to both the static and dynamic pressure changes within kilopascal (kPa) to megapascal (MPa) range, which depended on the modulus of the matrix. Such unique features realized the non-contact optical measurement of surface pressure in hydrodynamics application.

2. Experimental section

2.1. Materials

Tetra(4-nitrophenyl) ethylene (TPE-4N) was obtained from Alpha Chemical Co., LTD (Henan, China). The Expancel Microspheres (Expancel® 093 DU 120) were purchased from Nouryon (Sweden),

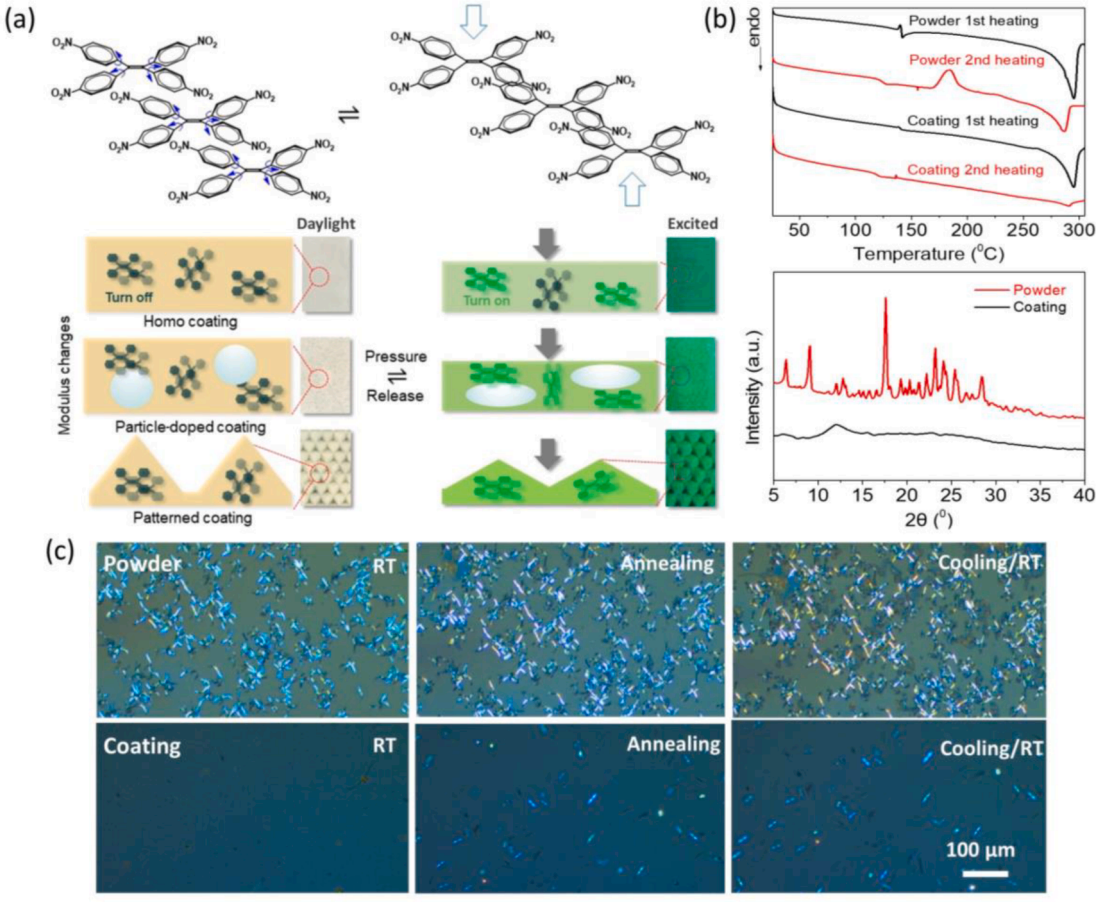

Fig. 1. (a) Chemical structure of TPE-4N, schematic illustration of the construction of AIE-based pressure sensitive coatings (AIE-PSP) with homogenously dispersed TPE-4N (Homo coating), or additionally doped by Expancel® particles (Particle-doped coating) and with a patterned surface (Patterned coating), and optical photographs of the coatings in daylight and under excitation at 365 nm. (b) DSC diagrams (up) of TPE-4N powder and a TPE-4N dispersed PDMS with 33 wt% of dye loading, and XRD (bottom) of TPE-4N powder and the as-prepared AIE-PSP homo coating containing 0.3 wt% of TPE-4N to the total PDMS mass. (c) Polarization microscopy of TPE-4N powder (coated on glass slide) and the spin-coated AIE-PSP homo coating with 0.2 wt% of dye loading at room temperature (RT, 25 °C), after annealing at 80 °C, and cooled down to RT again. The homo coating was not seriously cured before the start of observation to allow in situ crosslinking during annealing.

foamed at 175 °C for 10 min before use. High transparent optical adhesive potting adhesive poly(dimethyl-methylvinylsiloxane) prepolymer (PDMS, 184 Silicone elastomer, Sylgard) and silicone elastomer curing agent (Sylgard) were purchased from Dow Corning (Michigan, USA). Room-temperature vulcanizing silicone rubber (RTV) was obtained from Momentive/GE Toshiba (New York, USA). A derivative of dithienobenzothiadiazole was synthesized according to literature [44], for using as a reference dye without showing AIE characteristic.

2.2. Fabrication of the AIE-based pressure sensitive coatings (AIE-PSP)

Desired amount of TPE-4N was dissolved in chloroform (300 μL) by ultrasonic dispersion. To this PDMS (2 g) was added and stirred. Then silicone elastomer curing agent (0.1 g) was added to the above mixture. After intensive mixing and bubble removal in vacuum, the mixture was poured onto a substrate (such as a glass slide) to prepare the AIE-PSP coating with uniform thickness by scraping (KTQ-III, Ark instruments, China) or spin-coating (KW-4A, China), followed by curing at 100 °C for 3 h. During the procedure, weighted amount of foamed Expancel Microspheres could be mixed to the PDMS mixture before the addition of the curing agent, in order to prepare the particle-doped coatings. To prepare a surface patterned coating, a pyramid patterned mold was used instead of the planar substrate, with other steps kept as the same. In addition, AIE-PSP coatings with RTV as the elastic matrix were also prepared following the same procedure to test the generality of the fabrication route.

2.3. Characterizations

Differential scanning calorimetry (DSC) data was recorded on a differential scanning calorimeter (TA Instruments, Q2000, USA) under nitrogen at a heating rate of 10 °C/min. After cooling at a same rate, i.e. 10 °C/min, the second scanning test was carried out. For the DSC test, AIE-PSP sample was made by directly dispersing TPE-4N powder, without dissolving by solvent, into PDMS in order to monitor the crystallization intendancy of melting dye molecules in the polymer matrix. And to improve signal-to-noise ratio, high mass fraction of TPE-4N at 33 wt% was loaded into the silicone. X-ray diffraction (XRD) measurements were conducted on a Rigaku X-ray diffractometer (ULTIMA IV) with an X-ray source of Cu Kα at 40 kV and 40 mA, at a scan rate of 5° (2θ) per 1 min. Polarizing optical microscopic (POM) images were captured by a Leica DM 2700P polarization microscope (Leica Microsystems, Wetzlar, Germany) coupled with a digital camera and a heating device (Linkam Scientific Instruments LTD, UK). Thin film of neat TPE-4N was prepared by spin-coating from its chloroform dispersion on a cover glass. Likewise, thin film of AIE-PSP coating containing 0.2 wt% of AIEgens to the polymer mass was prepared through spin-coating as well. During the observation, the AIE-PSP coating or the dye film was heated by the heating device. And the AIE-PSP coating was compressed by pressing the cover glass using tweezers to realize pressurization-decompression cycles. Pictures around the same area of the sample surface were taken. The compressive modulus of the coatings was determined using INSTRON Model 5967 machine at room temperature in air. The AIE-PSP samples were cut to regular rectangles and the compression rate was 1 μm/s.

2.4. Fluorescence spectrophotometery

The fluorescence spectra were recorded by a fluorescence spectrophotometer (Techcomp FL970, China) with a temperature-controlled sample holder. The excitation wavelength was 365 nm and the reflected fluorescence signals were recorded. The coating was cut into 5 × 5 mm which was placed between two quartz clips. The distance of the two clips could then be adjusted by screwing the thread of holder to a predetermined scale, and thus a desired amplitude of compressive strain was gained. The pressure loaded on coating can be calculated by correlating the compressive strain with the modulus of the coating measured by the INSTRON. The force loading and unloading cycles were achieved by clamping and loosening the holder. Emission spectra were collected at different temperatures and under various compression. For checking the photostability, the time scanning mode was applied. The coating was continuously irradiated at 365 nm, while the emission at 525 nm was recorded.

2.5. Static pressure calibration

The relationship between static water pressure and emission intensity of the coatings was conducted by placing the coating on the bottom of a transparent cylinder, filled by water and subsequently compressing using a plunger. The cylinder was vertically put in a self-made heat preservation device. And the coating were excited from the bottom by a LED lamp (SJUV 4D-104, SJMAEA, China) with a central wavelength of 365 nm. Pictures taken using a CCD camera (FASTCAM Mini AX 200, Japan) equipped with a 420 nm long pass filter.

2.6. Dynamic surface pressure distribution

Falling ball experiment was carried out by leaving a 22.5 g round ball to roll down from the top edge of an AIE-PSP coating with a size of 3 × 5 cm, placed on a transparent heating plate with a slope of 7°. The coating was heated to 80 °C. A UV lamp and a high-speed CCD camera were placed on the bottom for tracing the trail of the traveling ball.

To monitor the surface pressure distribution in underwater environment, rudder and cylindrical models were made of which the vertical surface was covered by the AIE-PSP coating. The model was fixed on a long water tank with a slope of 15°, and immersed in water. The temperature of equipment, i.e. water in tank, was hold at 80 °C throughout the experiment. By opening the drain pipe at the end of the tank, water started to flow across the model. The coating was excited by the LED lamp and monitored by the high-speed CCD camera which were placed outside the transparent water bank.

The collected images were analyzed and pseudocolor processed using Image J and Image-Pro Plus 6.0 software following the software's introduction.

3. Results and discussion

3.1. Preparation of AIE-PSP coatings

The AIE-based pressure sensitive coatings (AIE-PSP) were prepared by dispersing AIEgen inside a silicone matrix, e.g. PDMS elastomer. TPE-4N was selected as the AIEgen because it is highly emissive as amorphous powder [12]. On the other hand, in order to tune the elastic modulus of the coatings without differing the microenviroment of dye molecules, except the production of homogeneous silicone film (homo coating), the expanded thermoplastic microspheres, i.e. Expancel Microspheres (diameter 120 μm after foaming), were used for the preparation of particle-doped coating, and pyramidal pattern was conducted on the surface of the silicone to gain a patterned coating. The optical pictures of the coatings are plotted in Fig. 1**a**, in which the AIE-PSP films emit mild green light under an excitation at 365 nm, indicating the homogeneous dispersion of the dye in the silicone. The thickness of the coatings was tunable during the preparation. Homo, particle-doped and patterned coatings with thickness of 650 μm, 800 μm and 2.3 mm respectively were used in the following investigations unless otherwise mentioned.

The condensed state of TPE-4N in the silicone matrix was assessed by DSC, XRD and POM. Fig. 1**b** shows that the powder shaped TPE-4N reagent is highly crystallized, demonstrating a melting temperature of 290 °C in the DSC curve. And the quenched sample appears a cold-crystallization peak at 184 °C during the second heating process, and subsequently displays a melting peak with 66% of the initial area in the

first scan (Fig. 1**b**), exhibiting high crystallization tendency of the dye molecules. Besides, TPE-4N powder also exhibits a glass transition temperature (T_g) at ca. 130 °C, indicating that the mobility of the dye is restricted at lower temperature [45]. Differently, the second scan of dye powder doped PDMS film only displays slight endothermic peak, ca. 15% compared to that in the first scan of the as-prepared film, whilst the later has a melting enthalpy similar as the TPE-4N powder (Fig. 1**b**). The results infer that the crystallization of TPE-4N can be significantly prohibited by the silicone matrix due to the confinement effect of the polymer network on the movement of the dye molecules. XRD also shows rather weak signals from the AIE-PSP coating associated with the broad peak of silicone in contrast to the strong diffractions from the powders (Fig. 1**b**). Nevertheless, it is noted that the dye molecules are able to reserve an aggregate state in the film since in DSC the onset of T_g from the dye doped film is similar to that of powder sample even in the second scan. To further clarify this, AIE-PSP coating containing 0.2 wt% of TPE-4N was freshly made for in situ POM observation. During curing at 80 °C, a few anisotropic optical textures started to be revealed, but with much less density and very different morphology in comparison with the interference patterns of the neat TPE-4N (Fig. 1**c**). Such pictures imply that the generation of the silicone meshes has induced the gathering of the AIEgens, but not led to crystallization, which eventually caused the formation of packed clusters [46,47], owing to the steric hindrance of polymer network that has prevented the dye molecules from wide-scale motion at the temperature below T_g.

3.2. Fluorescence property of AIE-PSP coatings

The fluorescence property of AIE-PSP coatings is shown in Fig. 2. The powder form TPE-4N displays a maximum absorbance at 450 nm in the excitation spectrum and an emission entered at 525 nm (Fig. 2**a**). However for the homo coatings, Fig. 2**b** shows that the excitation peak is at 450 nm only when the coating contains the highest AIEgen amount, i.e. 1.2 wt% to the total mass of PDMS, but shifts hypsochromically following the decrease of dye concentration, i.e. from 0.6 wt% to 0.2 wt %. In contrast, the emission peak keeps at 525 nm for all samples except that with the highest AIEgen content, which appears at 520 nm, a position related to the crystallized structure of the dye [12]. Meanwhile, the fluorescence intensity reaches a maximum value wherever 0.2 wt% of TPE-4N were loaded in the coating (Fig. 2**c**). Such phenomena are attributed to the condensed state of the dye molecules in the silicone matrix. While the polymer network avoided serious crystallization of TPE-4N, not all dye molecules were molecularly dispersed in the silicone phase. As suggested by XRD and POM (Fig. 1), with certain amount of TPE-4N, e.g. 0.2–0.3 wt%, the AIEgens formed clusters in the polymer matrix, which endows the AIE activity. However, the spatial limitation of the mesh size prevented the formation larger conjugation with higher TPE-4N loading, but resulting in more closely-packed aggregates which could favor ISC [12], and hence the decreased fluorescence intensity (Fig. 2c). Meanwhile, the photostability of TPE-4N molecule was not influenced by the silicone matrix, showing similar thermal quenching effect and minor photobleaching as the neat TPE-4N (**Figs. S1 and S2**, Supporting Information).

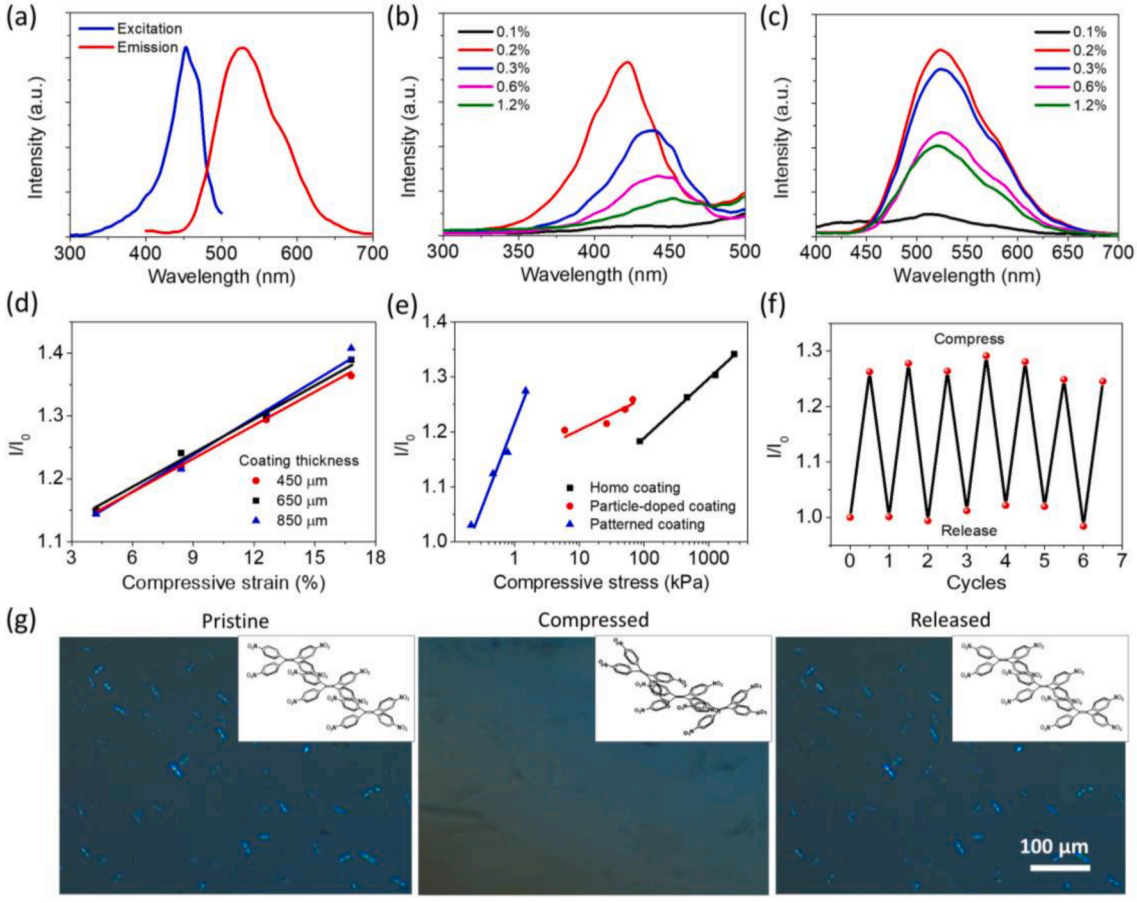

Fig. 2. (a) Excitation and emission spectra of TPE-4N powder. (b) Excitation spectra and (c) emission spectra of TPE-4N loaded PDMS coatings (homo coating) containing various weight percentage of the dye. (d) Influence of thickness on the pressure sensitivity (I/I_0) of homo coating containing 0.3 wt% of TPE-4N to the PDMS mass. (e) Influence of microstructure on the pressure sensitivity of AIE-PSP coatings containing 0.3 wt% of TPE-4N. (f) Reversibility of the homo coating (containing 0.3 wt% of TPE-4N) in the pressure loading–unloading cycles. The above measurements (a-f) were carried out at room temperature (25 °C), and λ_{ex} = 365 nm, λ_{em} = 525 nm where applicable. (g) Polarization microscopy of the homo coating in a pressure loading–unloading cycle at 80 °C.

The pressure dependence of fluorescence of the AIE-PSP coatings was then tested at temperatures from 25 °C to 80 °C under different amplitude of compression. Luminescent enhancement was observed on all three kinds of coatings (**Fig. S3**). And it is recognized that in this regime, the level of fluorescence increase (I/I_0), defined as the fluorescence intensity at 525 nm under applied pressure (I) to that under atmospheric pressure (I_0), is determined by the level of compressive strain on the AIE-PSP coatings, as evidenced by the fact that changing the coating thickness caused almost no change of the I/I_0 value (Fig. 2**d**). As a result, the pressure sensitivity of the coatings depends on their compressive modulus. From the stress–strain curves (**Fig. S4**), the compressive modulus of the particle-doped coating and the patterned coating is determined to be 480 kPa and 16 kPa, in comparison with 1.4 MPa of the homo coating. Accordingly, these coatings response to different surface pressure stimulation, ranged from kPa to MPa, converted from strain to stress (Fig. 2**e**). The calculated pressure sensitivity is 3.6 %/MPa, 0.1 %/kPa and 18.5 %/kPa of fluorescence difference for the homo, particle-doped and patterned coatings, respectively. The results suggest that the sensing capacity of the pressure sensor can be personalized by adjusting the mechanical property of the coating.

Reversibility is crucial for MRL materials. In this work, the intensity variation of the AIE-PSP coatings is highly reversible with the alternation of compressive strain and relaxation (Fig. 2**f**, **Fig. S5 and Movie S1**, Supporting Information), which is attributed to the elasticity of the PDMS matrix as well as the amorphous and aggregate characteristics of the dye. While the polymer meshes kept TPE-4N in amorphous state, the quantum yield of the emission depends on the rotation or the vibration ability of the aggregated dye molecules in the polymer meshes, i.e. the extent of RIM, relating to the excited-state energy consumption [15,34]. Since physical deformation of the polymer network affects the dye packing and hence the amplitude of the dye motion, the luminescence behavior varies accordingly. Furthermore, with the elastic nature, the deformation of PDMS is recoverable, which drives the reversible change of the fluorescence intensity within compression-decompression cycles. As observed by in situ POM, the light spots shown in the AIE-PSP coating disappear under pressure and reappear soon after the release of force loading (Fig. 2**g**), which infers that the compacted distance between AIEgens could be reopened after the removal of compression. Besides, in amorphous state, the conformation of the dye is gradually altered following the process of the network deformation, so that the fluorescence changes continuously with the extent of strain, or the level of the applied pressure on the coating surface. This allows the functional relationship fitting between the pressure and the emission intensity within proper range of strain (Fig. 2**e**). To further demonstrate the role of the polymer matrix, we alternated PDMS by another kind of elastomer to prove the generality of the rationale. Using RTV as the matrix, we confirmed that the fluorescence increase (I/I_0) of the embedded TPE-4N could follow a linear relation with the applied compressive strain (**Fig. S6**).

It was also found that the temperature influenced the sensitivity of AIE-PSP coatings. As to the patterned coating, I/I_0 increases to 1.8 at 80 °C in comparison with 1.3 at 25 °C under the same strain of 10 %

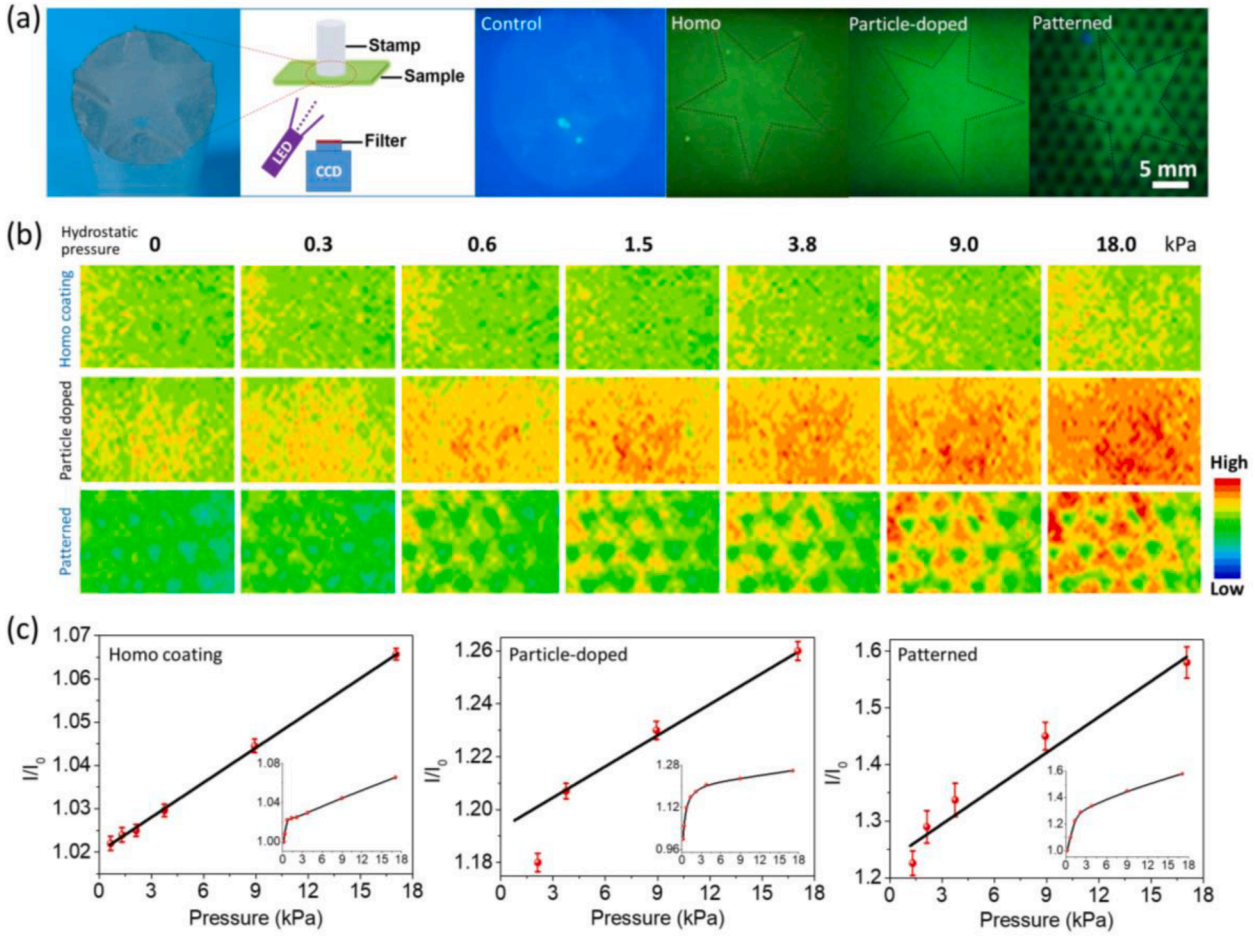

Fig. 3. (a) Demonstration of the AIE-PSP coatings (containing 0.3 wt% of TPE-4N) to respond local mechanical pressure loaded by placing a stamp on the coating surface. (b) Pseudo color pictures taken from the AIE-PSP coatings in response to the loaded hydrostatic pressures. (c) Calibration of the fluorescence intensity variation (I/I_0) as a function of the loaded hydrostatic pressure on the coating surface as shown in (b). I_0 is the averaged fluorescence intensity from selected pixels under atmospheric pressure and I is the averaged fluorescence intensity under the applied pressure. λ_{ex} = 365 nm and the temperature of the coatings was 80 °C.

(Fig. S7), mainly attributed to lower I_0 of TPE-4N at higher temperature (Fig. S1). Thus, the measurements at a high temperature, e.g. 80 °C, will favor the record of pressure change as well as the image processing. In this case, the influence of temperature on the compressive modulus of the polymer matrix should be taken in account for the stress–strain correlation.

3.3. Pressure responsiveness of AIE-PSP coatings

To demonstrate the pressure imaging ability, a stamp of pentagram was placed on the surface of the AIE-PSP coatings on a glass substrate. The coatings were then excited and monitored from the bottom through the glass slide. Even from optical pictures (Fig. 3**a**), the enhancement of fluorescence can be clearly revealed in the area under the shape of pentagram. In contrast, the control sample with the reference dye cannot recognize the change of local static pressure via fluorescence imaging. This substantiates that the optical imaging was obtained from the emission increment of TPE-4N instead of the variation of coating thickness. The mass of stamp is 31.5 g, providing a pressure of ca. 2.5 kPa, inferring that the AIE-PSP coatings have distinguished very slight compression.

The pressure sensitivity of the coatings was quantitatively calibrated by hydrostatic calibration at 80 °C. By a step-loading of hydrostatic pressure up to 18 kPa, the color change from the pseudo color pictures is clearly seen (Fig. 3**b**). It is recognized that the color difference becomes more obvious in the patterned and the particle-doped coatings, in agreement with the responsiveness of the samples, which are more sensitive to the stress within the kPa range. After calculating the pixel values in a particular area, the relationship between the fluorescence intensity and the applied pressure is plotted in Fig. 3**c**. Just like the fluorescence measurements (Fig. 2**e**), the averaged I/I_0 is monotonically increasing with the pressure value, although it is not showing a linear relationship throughout the pressure range. Nevertheless, the calibration supports the possibility to record pressure value at any pixel in the picture, and therefore ensures the capability of the coatings to image the surface pressure distribution in 2D.

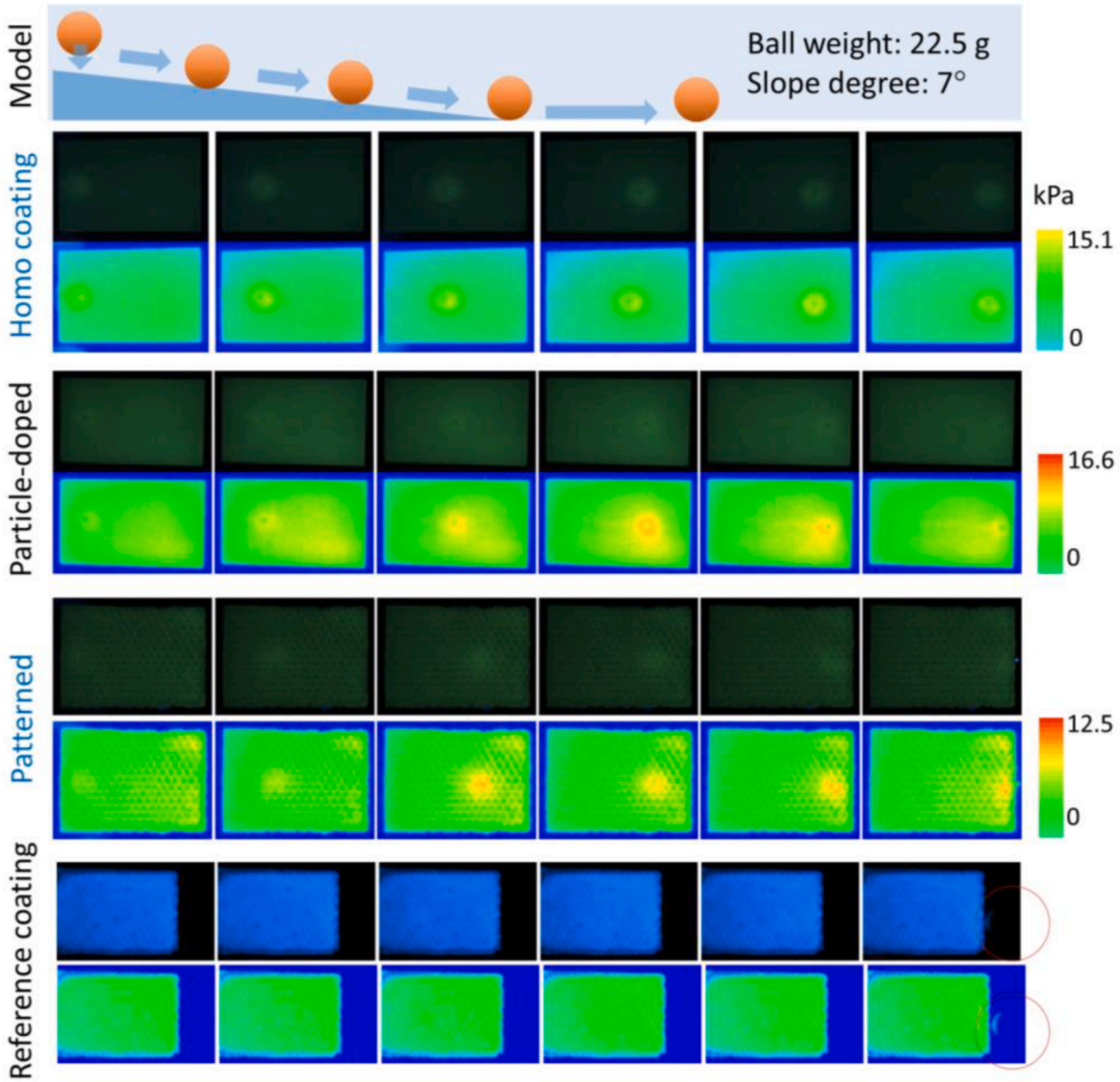

Fig. 4. Continuous photo shooting from the back surface of the AIE-PSP coatings (containing 0.3 wt% of PET-4N) in the process of the falling ball experiment. For each coating, the upper row shows the optical images and bottom shows the pseudo color images. The red circles indicate the position of the ball in the image. λ_{ex} = 365 nm and the temperature of the coating was 80 °C. The movement of the ball on the coatings can be viewed from **Movie S2**. (For interpretation of the references to color in this figure legend, the reader is referred to the web version of this article.)

3.4. Surface pressure imaging in dynamic processes

In addition to the static sensing, the AIE-PSP coatings were also tested for monitoring an unsteady compression process. Falling ball experiment was performed to evaluate the capacity of the coatings to detect the dynamical evolution of mechanical force on the surface. The results are shown in Fig. 4. Both optical images and the produced pseudo color photos recorded the moving of the ball on the sensitive coatings within a period of less than 1 s, while no signal was observed from the reference coating. More important, round-shaped patterns were seen in all pictures, which indicates a fast dynamics of the mechanoluminescent process because the fluorescence enhancement in the previously compressed area had been self-recovered sooner after the ball was rolling away (**Movie S2**). This once again corroborates the ideal reversibility of the mechanoluminescence performance gained by the AIE-PSP coatings. The recovery time is measured in subsecond level. Such responsiveness will benefit the utility of the coatings on dynamic pressure measurement.

To further examine the application of the AIE-PSP coatings, an underwater test was carried out to observe the surface pressure variation on a rudder model when facing a water flow (Fig. 5). Particle-doped coating and surface patterned coating were chosen for the test due to higher sensitivity. The AIE-PSP coatings were covered on the lateral surface of the model (**Fig. S8**). Compared to the static state, one can see the enhancement of surface pressure in the front part and the upper region of the underwater model after the water started to flow (Fig. 5). This is reasonable because the forward edge of the rudder was affording the water drag. Besides, it is not surprising that the patterned coating obtained more distinguishable high-pressure zone since the water flow should not only cause vertical deformation on the surface, but also lead to the bending of the pyramidal bulges. The heterogeneity deformation of the matrix, i.e. in both uniaxial and lateral directions, would cause the change of dye conformation in greater amplitude which thus resulted in larger difference on the fluorescence intensity. Besides, it should be also pointed out that with water draining, the model started to resurface over water with the drop of waterline. In this case, the temperature of the coating decreased from 80 °C to room temperature, which also led to the increase of fluorescence intensity, as demonstrated in the rightmost pseudo color images in Fig. 5. Thus, under the experimental condition, only pressure distribution below the waterline could be properly monitored without correction. To further exploit the measurement to the overwater part of the model, dual-luminophore regimes with the inclusion of a thermo-sensitive reference dye will be necessary. Despite these, the experimental results obviously suggest the ability of the AIE-PSP coatings as an optical sensor to measure both isotropic compression and anisotropic pressure distribution on the surface. A cylindrical model was used to show the generality of the coatings in the measurement (**Fig. S9**).

4. Conclusions

In this work, we developed AIE-based MRL polymeric coatings to

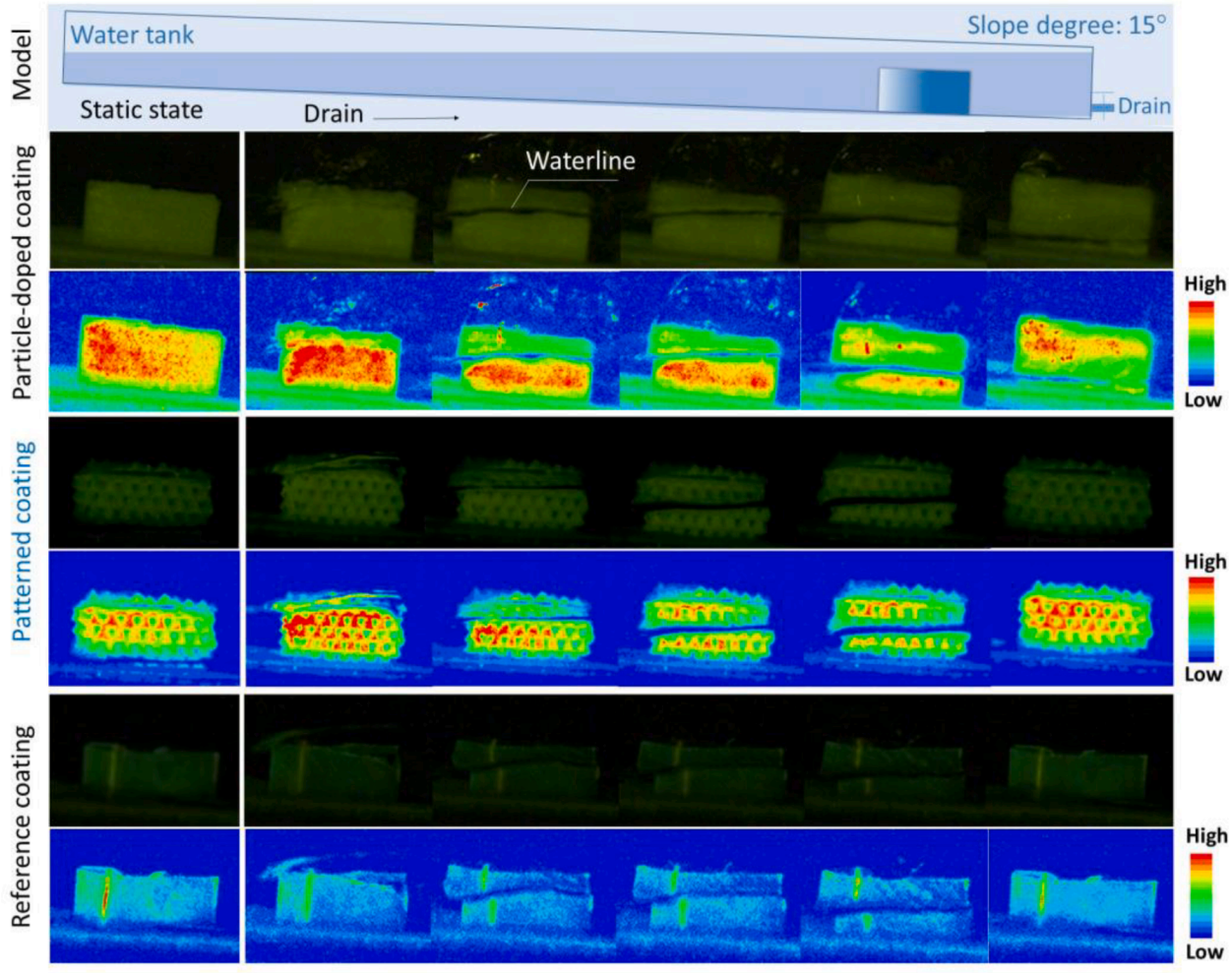

Fig. 5. Pressure distribution on the vertical wall of a rudder shaped model monitored by AIE-PSP coatings during water flowing through. The upper row, optical images; the bottom row, pseudo color images. λ_{ex} = 365 nm and the temperature of the water was 80 °C.

realize the non-contact optical surface pressure measurement for hydrodynamics research. The pressure sensitive coatings are composed of an elastomer matrix and the embedded AIEgens, which show a mechanoluminescent characteristic against compression. The rationale is that the polymer chains restricted the crystallization of the AIEgens and kept them in an amorphous aggregate state. Therefore, the mechanoresponse of photoluminescence is driven by the conformation change of the dye molecules, directly caused by the strain of the polymer network. As a result, the responsiveness of the pressure sensor is determined by the mechanical property of the polymer coating, namely the modulus of the PMDS matrix, which contributes to the high pressure sensitivity in kPa to MPa range, the ideal reversibility in force loading–unloading cycles and the preferable ability for quantitative determination of loaded stress. These features allowed the AIE-PSP coatings to monitor surface pressure distribution in both static and dynamic processes as well as in underwater condition. Such kind of pressure sensors would have wide applications for example in industrial manufacturing, healthcare and environment detecting.

Declaration of Competing Interest

The authors declare that they have no known competing financial interests or personal relationships that could have appeared to influence the work reported in this paper.

Acknowledgments

The work was financially supported by the National Natural Science Foundation of China (51873214) and the Fundamental Research Funds for the Central Universities.

Appendix A. Supplementary data

Supplementary data to this article can be found online at https://doi.org/10.1016/j.cej.2021.133449.

References

[1] C. Bermejo, F. Haerizadeh, H. Takanaga, D. Chermak, W.B. Frommer, Optical sensors for measuring dynamic changes of cytosolic metabolite levels in yeast, Nat. Protoc. 6 (2011) 1806–1817.
[2] R.N. Conmy, P.G. Coble, J. Farr, A.M. Wood, K. Lee, W.S. Pegau, I.D. Walsh, C. R. Koch, M.I. Abercrombie, M.S. Miles, M.R. Lewis, S.A. Ryan, B.J. Robinson, T. L. King, C.R. Kelble, J. Lacost, Submersible optical sensors exposed to chemically dispersed crude oil: wave tank simulations for improved oil spill monitoring, Environ. Sci. Technol. 48 (2014) 1803–1810.
[3] X. Jiang, H. Gao, X. Zhang, J. Pang, Y. Li, K. Li, Y. Wu, S. Li, J. Zhu, Y. Wei, L. Jiang, Highly-sensitive optical organic vapor sensor through polymeric swelling induced variation of fluorescent intensity, Nat. Commun. 9 (2018) 3799.
[4] D. Peng, J. Chen, L. Jiao, Y. Liu, A fast-responding semi-transparent pressure-sensitive paint based on through-hole anodized aluminum oxide membrane, Sensor. Actuat. A-Phys. 274 (2018) 10–18.
[5] R. Jia, W. Tian, H. Bai, J. Zhang, S. Wang, J. Zhang, Amine-responsive cellulose-based ratiometric fluorescent materials for real-time and visual detection of shrimp and crab freshness, Nat. Commun. 10 (2019) 795.
[6] G. Singh, S.P. Pandey, P.K. Singh, A dual intensity and lifetime based fluorescence sensor for perrhenate anion, Sensor. Actuat. B-Chem. 330 (2021), 129346.
[7] D. Yang, J. Li, J. Ren, Q. Wang, S. Zhou, Q. Wang, Z. Xie, X. Qu, Fast-response oxygen sensitive transparent coating for inner pressure ratiometric optical mapping, J. Mater. Chem. C 9 (2021) 3919–3927.
[8] T. Han, L. Liu, D. Wang, J. Yang, B.Z. Tang, Mechanochromic fluorescent polymers enabled by AIE processes, Macromol. Rapid Commun. 42 (2021) 2000311.
[9] D. Yang, J. Ren, J. Li, Q. Wang, Q. Wang, Z. Xie, X. Qu, Construction of bi-layer biluminophore fast-responding pressure sensitive coating for non-contact unsteady aerodynamic testing, Polym. Test. 77 (2019), 105922.
[10] T. Liu, J.P. Sullivan, Pressure and Temperature Sensitive Paints, Springer, Berlin, Heidelberg, 2005.
[11] J. Chen, Y. Liu, D. Peng, A bio-inspired functional film embedded with fluorescent elastic microspheres for pressure sensing, Appl. Phys. Lett. 116 (2020), 123701.
[12] W. Zhao, Z. He, Q. Peng, J.W.Y. Lam, H. Ma, Z. Qiu, Y. Chen, Z. Zhao, Z. Shuai, Y. Dong, B.Z. Tang, Highly sensitive switching of solid-state luminescence by controlling intersystem crossing, Nat. Commun. 9 (2018) 3044.
[13] E. Ubba, Y. Tao, Z. Yang, J. Zhao, L. Wang, Z. Chi, Organic mechanoluminescence with aggregation-induced emission, Chem. Asian J. 13 (2018) 3106–3121.
[14] H. Traeger, D.J. Kiebala, C. Weder, S. Schrettl, From molecules to polymers-harnessing inter- and intramolecular interactions to create mechanochromic materials, Macromol. Rapid Commun. 42 (2021) 2000573.
[15] X. Wang, C. Qi, Z. Fu, H. Zhang, J. Wang, H.T. Feng, K. Wang, B. Zou, J.W.Y. Lam, B.Z. Tang, A synergy between the push-pull electronic effect and twisted conformation for high-contrast mechanochromic AIEgens, Mater. Horiz. 8 (2021) 630–638.
[16] J. Zhang, B. He, Y. Hu, P. Alam, H. Zhang, J.W.Y. Lam, B.Z. Tang, Stimuli-responsive AIEgens, Adv. Mater. 33 (2021) 2008071.
[17] M. Zhang, J. Wei, Y. Zhang, B. Bai, F. Chen, H. Wang, M. Li, Multi-stimuli-responsive fluorescent switching properties of anthracene-substituted acylhydrazone derivative, Sensor. Actuat. B-Chem. 273 (2018) 552–558.
[18] P. Shi, D. Deng, C. He, L. Ji, Y. Duan, T. Han, B. Suo, W. Zou, Mechanochromic luminescent materials with aggregation-induced emission: mechanism study and application for pressure measuring and mechanical printing, Dyes Pigments 173 (2020), 107884.
[19] R. Taniguchi, T. Yamada, K. Sada, K. Kokado, Stimuli-responsive fluorescence of AIE elastomer based on PDMS and tetraphenylethene, Macromolecules 47 (2014) 6382–6388.
[20] S.A. Sharber, A. Mann, K.C. Shih, W.J. Mullin, M.P. Nieh, S.W. Thomas III, Directed polymorphism and mechanofluorochromism of conjugated materials through weak non-covalent control, J. Mater. Chem. C 7 (2019) 8316–8324.
[21] S.A. Sharber, K.C. Shih, A. Mann, F. Frausto, T.E. Haas, M.P. Nieh, S.W. Thomas, Reversible mechanofluorochromism of aniline-terminated phenylene ethynylenes, Chem. Sci. 9 (2018) 5415–5426.
[22] P. Sudhakar, K.K. Neena, P. Thilagar, H-Bond assisted mechanoluminescence of borylated aryl amines: tunable emission and polymorphism, J. Mater. Chem. C 5 (2017) 6537–6546.
[23] Y. Dong, J. Zhang, A. Li, J. Gong, B. He, S. Xu, J. Yin, S. Hua Liu, B.Z. Tang, Structure-tuned and thermodynamically controlled mechanochromic self-recovery of AIE-active Au(I) complexes, J. Mater. Chem. C 8 (2020) 894–899.
[24] T. Wang, N. Zhang, K. Zhang, J. Dai, W. Bai, R. Bai, Pyrene boronic acid cyclic ester: a new fast self-recovering mechanoluminescent material at room temperature, Chem. Commun. 52 (2016) 9679–9682.
[25] M. Ikeya, G. Katada, S. Ito, Tunable mechanochromic luminescence of 2-alkyl-4-(pyren-1-yl)thiophenes: controlling the self-recovering properties and the range of chromism, Chem. Commun. 55 (2019) 12296–12299.
[26] Y. Sagara, H. Traeger, J. Li, Y. Okado, S. Schrettl, N. Tamaoki, C. Weder, Mechanically responsive luminescent polymers based onsupramolecular cyclophane mechanophores, J. Am. Chem. Soc. 143 (2021) 5519–5525.
[27] H. Traeger, Y. Sagara, D.J. Kiebala, S. Schrettl, C. Weder, Folded perylene diimide loops as mechanoresponsive motifs, Angew. Chem. Int. Ed. 60 (2021) 16191–16199.
[28] G. Zhang, J. Lu, M. Sabat, C.L. Fraser, Polymorphism and reversible mechanochromic luminescence for solid-state difluoroboron avobenzone, J. Am. Chem. Soc. 132 (2010) 2160–2162.
[29] T. Butler, A.S. Mathew, M. Sabat, C.L. Fraser, Camera method for monitoring a mechanochromic luminescent β-diketone dye with rapid recovery, ACS Appl. Mater. Interfaces 9 (2017) 17603–17612.
[30] P. Alam, N.L.C. Leung, Y. Cheng, H. Zhang, J. Liu, W. Wu, R.T.K. Kwok, J.W. Y. Lam, H.H.Y. Sung, I.D. Williams, B.Z. Tang, Spontaneous and fast molecular motion at room temperature in the solid state, Angew. Chem. Int. Ed. 58 (2019) 4536–4540.
[31] H. Wu, C. Hang, X. Li, L. Yin, M. Zhu, J. Zhang, Y. Zhou, H. Ågrenc, Q. Zhang, L. Zhu, Molecular stacking dependent phosphorescence-fluorescence dual emission on single luminophore for self-recoverable mechanoconversion of multicolor luminescence, Chem. Commun. 53 (2017) 2661–2664.
[32] P.S. Hariharan, N.S. Venkataramanan, D. Moon, S.P. Anthony, Self-reversible mechanochromism and thermochromism of a triphenylamine-based molecule: tunable fluorescence and nanofabrication studies, J. Phys. Chem. C 119 (2015) 9460–9469.
[33] S. Ito, T. Taguchi, T. Yamada, T. Ubukata, Y. Yamaguchi, M. Asami, Indolylbenzothiadiazoles with varying substituents on the indole ring: a systematic study on the selfrecovering mechanochromic luminescence, RSC Adv. 7 (2017) 16953–16962.
[34] J. Mei, N.L.C. Leung, R.T.K. Kwok, J.W.Y. Lam, B.Z. Tang, Aggregation-induced emission: together we shine, united we soar!, Chem. Rev. 115 (2015) 11718–11940.
[35] D. Duc La, S.V. Bhosale, L.A. Jones, S.V. Bhosale, Tetraphenylethylene-based AIE-active probes for sensing applications, ACS Appl. Mater. Interfaces 10 (2018) 12189–12216.
[36] X. Yao, Z. Chi, Piezochromic aggregation-induced emission materials, Sci. China Chem. 43 (2013) 1090–1104.
[37] Y. Dong, B. Xu, J. Zhang, X. Tan, L. Wang, J. Chen, H. Lv, S. Wen, B. Li, L. Ye, B. Zou, W. Tian, Piezochromic luminescence based on the molecular aggregation of 9,10-Bis((E)-2-(pyrid-2-yl)vinyl)anthracene, Angew. Chem. Int. Ed. 51 (2012) 10782–10785.
[38] H. Yuan, K. Wang, K. Yang, B. Liu, B. Zou, Luminescence properties of compressed tetraphenylethene: the role of intermolecular interactions, J. Phys. Chem. Lett. 5 (2014) 2968–2973.
[39] A. Pucci, Mechanochromic fluorescent polymers with aggregation-induced emission features, Sensors 19 (2019) 4969.
[40] G. Iasilli, A. Battisti, F. Tantussi, F. Fuso, M. Allegrini, G. Ruggeri, A. Pucci, Aggregation-induced emission of tetraphenylethylene in styrene-based polymers, Macromol. Chem. Phys. 215 (2014) 499–506.

[41] I. Bronshtein, H. Weissman, I. Kaplan-Ashiri, B. Rybtchinski, Crystallization of small organic molecules in a polymer matrix: multistep mechanism enables structural control, Small 15 (2019) 1902936.
[42] S. Baghel, H. Cathcart, N.J. O'Reilly, Polymeric amorphous solid dispersions: a review of amorphization, crystallization, stabilization, solid-state characterization, and aqueous solubilization of biopharmaceutical classification system class II drugs, J. Pharm. Sci. 105 (2016) 2527–2544.
[43] T. Cai, L. Zhu, L. Yu, Crystallization of organic glasses: effects of polymer additives on bulk and surface crystal growth in amorphous nifedipine, Pharm. Res. 28 (2011) 2458–2466.
[44] A. Efrem, C.J. Lim, Y. Lu, S.C. Ng, Synthesis and characterization of dithienobenzothiadiazole-based donor-acceptor conjugated polymers for organic solar cell applications, Tetrahedron Lett. 55 (2014) 4849–4852.
[45] M. Más-Montoya, R.A.J. Janssen, The effect of H- and J-Aggregation on the photophysical and photovoltaic properties of small thiophene-pyridine-dpp molecules for bulk-heterojunction solar cells, Adv. Funct. Mater. 27 (2017) 1605779.
[46] W.Z. Yuan, Z.Q. Yu, P. Lu, C. Deng, J.W.Y. Lam, Z. Wang, E. Chen, Y. Ma, B. Z. Tang, High efficiency luminescent liquid crystal: aggregation-induced emission strategy and biaxially oriented mesomorphic structure, J. Mater. Chem. 22 (2012) 3323–3326.
[47] X. Li, W. Hu, Y. Wang, Y. Quan, Y. Cheng, Strong CPL of achiral AIE-active dyes induced by supramolecular self-assembly in chiral nematic liquid crystals (AIE-N*-LCs), Chem. Commun. 55 (2019) 5179–5182.